The electric field dependent $g-$factor for the lead monofluoride, PbF, ground state

V.V. Baturo,[1,2] P. M. Rupasinghe,[3] T. J. Sears,[4] R. J. Mawhorter,[5] J.-U. Grabow,[6] and A.N. Petrov[1,2,*]

[1] *Saint Petersburg State University, St. Petersburg, 199034, Russia*
[2] *Federal state budgetary institution "Petersburg Nuclear Physics Institute", Gatchina, Leningrad district 188300, Russia*
[3] *Department of Physics, State University of New York at Oswego, Oswego, New York 13126, USA*
[4] *Department of Chemistry, Stony Brook University, Stony Brook, New York 11794-3400, USA*
[5] *Department of Physics and Astronomy, Pomona College, Claremont, California 91711, USA*
[6] *Gottfried-Wilhelm-Leibniz-Universität, Institut für Physikalische Chemie and Elektrochemie, Lehrgebiet A, Hannover, D-30167 Germany*

The electric field dependent $g-$factor and the electron electric dipole moment (eEDM)-induced Stark splittings for the lowest rotational levels of ^{207,208}PbF are calculated. Observed and calculated Zeeman shifts for ^{207}PbF are found to be in very good agreement. It is shown that the ^{207}PbF hyperfine sublevels provide a promising system for the eEDM search and related experiments.

Spectroscopic and theoretical work on the PbF molecule over more than three decades including[1–11] has been reported. Based on data at optical resolution,[2], Shafer-Ray et al.[4] predicted that the electric-field-dependent $g-$factor of the ground state of ^{208}PbF could cross zero at an electric field of 68 kV/cm. This led to the conclusion that PbF might provide a uniquely sensitive probe of the electric dipole moment of the electron, eEDM, d_e.

Working to verify this, subsequent spectroscopy at higher resolution by McRaven et al.[5] and theoretical analysis in Ref.[6] revealed a mis-assignment of the parity of the lowest rotational levels and confusion concerning the sign of the large ^{207}Pb Frosch-Foley d (= -$A_\perp$) hyperfine parameter in the optical work on ^{207}PbF.[2, 7] The reanalysis performed by Yang et al.[9] with corrected spectroscopic constants showed the $g-$factor of the ground-state ^{208}PbF unfortunately does not vanish. Nevertheless the very small $g-$factor in the $^2\Pi_{1/2}$ ground state of PbF reduces the sensitivity to stray magnetic fields by about a factor of 20 with regard to comparable $^2\Sigma$ molecules. This is a significant advantage in parity non-conservation studies.

Analytical expressions for electric-field-dependent $g-$factor were obtained[4, 9] for ^{208}PbF under the assumption that mixing of different rotational levels by electric field is not important. In this paper we take the mixing into account by numerical inclusion of a large number of rotational states and consider both odd and even mass Pb isotopologues of PbF.

^{208}Pb is the most abundant lead $I = 0$ isotope with 52% natural abundance, while ^{207}Pb has a nuclear spin $I = 1/2$ and a natural abundance of 22%. The existence of the lead nuclear spin in ^{207}PbF has a surprisingly strong effect on the Zeeman splittings in low-lying fine and hyperfine split levels that has major implications for experimental eEDM searches. It was shown by Alphei et al.[8] that a coincidental near-degeneracy of levels of opposite parity in the ground rotational state $J = 1/2$ for ^{207}PbF[12] takes place, caused by near cancellation of energy shifts due to omega-type doubling and the ^{207}Pb^{19}F magnetic hyperfine interactions. Thus ^{207}PbF has also been proposed as a promising candidate for both temporal variation of the fundamental constants [13] and anapole moment [8, 14] experiments .

This general utility of ^{207}PbF for a variety of parity non-conservation experiments offers an alternative path to spectroscopically probing states of different parity and can be further enhanced by working with excited vibrational levels in the ground electronic X_1 state [15]. The levels of opposite parity (^{207}PbF levels 3 and 4 Fig. 1 of Ref. [7]) are only 266 MHz apart for v=0 and drop about 33 MHz for each step up the vibrational ladder, potentially crossing with a gap of only $\sim \pm 20$ MHz around $v = 7$ and $v = 8$.

The knowledge of $g-$factors helps to control and suppress important systematic effects due to stray magnetic fields [16–18]. However, neither theoretical nor experimental data for $g-$factors of ^{207}Pb^{19}F for the field-free case or in an external electric field have been reported to date. The main purpose of the article is to fill this gap.

EXPERIMENTAL DETAILS

As described in detail in our earlier study[7], the rotational Zeeman spectra were taken at the Gottfried-Wilhelm-Leibniz-Universität Hannover using a Fourier-transform microwave (FTMW) spectrometer that exploits a coaxial arrangement of the supersonic jet and resonator axes (COBRA)[19]. The resulting sensitivity coupled with laser ablation[20] of elemental Pb in a neon carrier gas augmented with a few percent of SF_6 enabled the observation of strong and robust signals, which were essential to measuring the Zeeman effect data for both ^{208}PbF and ^{207}PbF. As already mentioned, due to a cancellation of spin and orbital contributions inherent in the

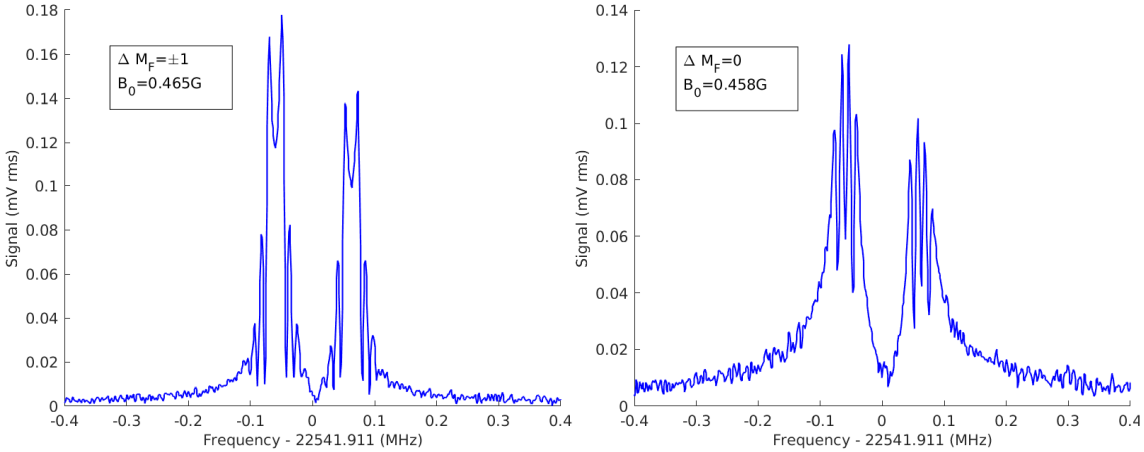

FIG. 1. (Color online) Rotational Zeeman spectra for the ^{207}PbF $F_L = 3/2 \rightarrow F_U = 5/2$ transition at 22541.912 MHz, showing the comparable (left) eight $\Delta M_F = \pm 1$ ($B_0 = 0.465$ G) and (right) four $\Delta M_F = 0$ ($B_0 = 0.458$ G) splittings, respectively. Note the doubled transitions due to the COBRA Doppler effect.

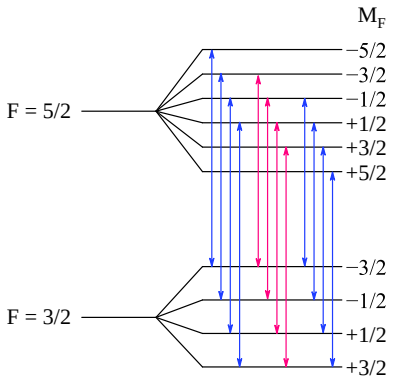

FIG. 2. (Color online) A depiction of rotational Zeeman spectra showed on Fig 1. The $\Delta M_F = \pm 1$ are marked by blue arrows The $\Delta M_F = 0$ components are marked by red arrows.

$^2\Pi$ ground state of PbF the observed Zeeman splittings are small. Even so, the excellent signal to noise with long emission decay times allows frequency measurements for unblended lines at an accuracy of 0.5 kHz and the resolution of transitions separated by more than 6 kHz. Figure 1 shows representative Zeeman spectra for the 22541.912 MHz transition in ^{207}PbF. Note that the resonance signals are doubled due to velocity structure in the experimental design. Figure 2 shows the transitions contributing to the spectra.

Given the high resolution of the jet spectra, the magnetic field calibration becomes the primary factor determining the uncertainty of the molecule-fixed $g-$factor, $G_\perp$. The currents in the 3 pairs of Helmholtz coils surrounding the chamber were independently varied to null out the magnetic field. This was done by adjusting the Helmholtz coil currents for all three pairs until all Zeeman splittings are minimized. Having full 3-axis control enabled the application of magnetic fields either perpendicular along two different axes or parallel to the radiation polarization. Having individual axis control, we can verify that the magnetic field in the sample region was indeed determined from the change in current in each coil. This was done by making independent experimental determinations of $G_\perp$, in both parallel and perpendicular configurations. They agreed to within about 2.5%, indicating that the uncertainty in our magnetic field calibration is approximately equal to the statistical error of our measurement.

Note that the initial experimental level assignments in Ref. [21] have been reversed, resulting in the completely consistent set of experimental and theoretical $G-$factors presented here. These are a factor of 1.45 smaller than used in Refs. [7, 8], and result in the prediction for the avoided level crossing discussed in Ref. [8] to occur at a magnetic field of approximately 1190 ± 80 G.

RESULTS AND DISCUSSION

The eigenvalues and eigenfunctions of the lead monofluoride molecule were obtained by numerical diagonalization of the Hamiltonian over the basis set of the electronic-rotational and nuclear spin wavefunctions. Details of the method and parameters of the Hamiltonian can be found in Refs. [10, 11, 22]. Parameters used include the body-fixed $g-$factors $G_\parallel = 0.081(5)$, $G_\perp = -0.27(1)$ [11], nuclear $g-$factors $g_{^{19}F} = 5.25772\mu_N$, $g_{^{207}Pb} = 1.18204\mu_N$ [23], and the body-fixed molecular dipole moment $D = 1.38$ a.u. [7]. Further details are provided in Refs. [7, 24].

TABLE I. Observed $(\Delta\nu/B)_{exp}$ (MHz/G) and calculated $(\Delta\nu/B)_{th}$ (MHz/G) Zeeman shifts of the $J = 1/2 \rightarrow J = 3/2$ transitions for PbF. $\Delta\nu$ is the difference between transition frequencies when magnetic field of value B is applied and field free case. The number in parenthesis gives a two standard deviation error in the final digits of precision. The subscripts L and U in F_L, F_U, MF_L, MF_U refer to the upper and lower energy level of the transition, respectively. F means the total (electronic plus rotational plus nuclear spins) momentum, MF its projection to the laboratory axis.

Unsplit line (MHz)	F_L	F_U	MF_L	MF_U	$(\Delta\nu/B)_{exp}$	$(\Delta\nu/B)_{th}$	$(\Delta\nu/B)_{exp} - (\Delta\nu/B)_{th}$
18333.501	3/2	5/2	3/2	1/2	−0.101(12)	−0.1121(60)	0.0111
			1/2	−1/2	−0.0755(30)	−0.0803(28)	0.0048
			−1/2	−3/2	−0.04984(45)	−0.0486(51)	−0.0012
			3/2	3/2	−0.0453(20)	−0.0475(83)	0.0022
			−3/2	−5/2	−0.01650(48)	−0.017(11)	0.001
			1/2	1/2	−0.0139(20)	−0.0157(27)	0.0018
			−1/2	−1/2	0.0159(20)	0.0160(28)	−0.0001
			3/2	5/2	0.01647(50)	0.017(11)	−0.001
			−3/2	−3/2	0.0474(20)	0.0475(83)	−0.0001
			1/2	3/2	0.05035(37)	0.0489(50)	0.0015
			−1/2	1/2	0.0763(47)	0.0805(28)	−0.0042
22541.912	3/2	5/2	−3/2	−1/2	−0.0957(35)	−0.0910(59)	−0.0047
			−1/2	1/2	−0.0689(21)	−0.0693(27)	0.0004
			1/2	3/2	−0.04727(76)	−0.0476(50)	0.0003
			−3/2	−3/2	−0.03326(83)	−0.0326(81)	−0.0007
			3/2	5/2	−0.02523(52)	−0.026(10)	0.001
			−1/2	−1/2	−0.01093(30)	−0.0109(27)	0.0000
			1/2	1/2	0.01062(48)	0.0109(28)	−0.0003
			−3/2	−5/2	0.02504(57)	0.026(10)	−0.001
			3/2	3/2	0.03316(76)	0.0326(82)	0.0006
			−1/2	−3/2	0.0466(10)	0.0475(49)	−0.0009
			1/2	−1/2	0.0675(26)	0.0692(27)	−0.0017
			3/2	1/2	0.0983(58)	0.0910(60)	0.0073
22658.902	1/2	3/2	−1/2	−3/2	−0.1448(10)	−0.1465(50)	0.0017
			−1/2	−1/2	−0.05157(74)[a]	−0.0500(17)	−0.0016
			1/2	−1/2	−0.0507(25)[a]	−0.0470(17)	−0.0037
			−1/2	1/2	0.05073(99)	0.0467(16)	0.0040
			1/2	1/2	0.0516(19)	0.0497(16)	0.0019
			1/2	3/2	0.14387(52)	0.1465(49)	−0.0026
22691.749	1/2	1/2	1/2	−1/2	−0.09555(46)	−0.1000(33)	0.0045
			−1/2	1/2	0.09819(81)	0.1003(32)	−0.0021

[a] Typographic error in [21], corrected here

The energy levels of interest for potential eEDM experiments on ^{208}PbF are the $F^p = 1^-$ and $F^p = 1^+$ states which are the first and fourth energy levels in zero field. $p = \pm 1$ means the parity of a state. For ^{207}PbF, the levels of interest are the closely spaced Ω-doublet states $F^p = 3/2^-$, $F^p = 1/2^-$, $F^p = 1/2^+$ and $F^p = 3/2^+$, which are the second, third, fourth and fifth energy levels. The relevant energy levels can be seen in Fig. 1 of Ref. [7]. In an eEDM search experiment opposite parity levels are mixed in an electric field to polarize the molecule. As the molecule becomes fully polarized the splitting ΔE_d between $\pm M_F$ levels due to eEDM related Stark shift reaches the maximum value $2d_e E_{\text{eff}}$, where $E_{\text{eff}} = 40$ GV/cm [25] is the effective internal electric field. Assuming eEDM value $|d_e| = 1.1 \times 10^{-29}$ from current limit [18] (ACME II experiment), we have $2d_e E_{\text{eff}} = 0.2$mHz. For any real electric field the splitting is less than $2d_e E_{\text{eff}}$ by an absolute value. In Fig. 3 the calculated eEDM induced Stark splittings for ^{208,207}PbF are presented.

The calculated and observed[21] Zeeman shifts of the $J = 1/2 \rightarrow J = 3/2$ transitions for ^{207}PbF are given in Table I and graphically in Fig. 4. The deviations between calculated and observed Zeeman shifts (E_{Z}) are consistent with the estimated experimental and theoretical uncertainties (δE_{Z}). Conservative theoretical uncertainties were calculated as

$$\delta E_{\text{Z}} = \sqrt{\left(\frac{\partial E_{\text{Z}}}{\partial G_{\parallel}}\delta G_{\parallel}\right)^2 + \left(\frac{\partial E_{\text{Z}}}{\partial G_{\perp}}\delta G_{\perp}\right)^2}, \qquad (1)$$

where $\delta G_{\parallel} = 0.005$, $\delta G_{\perp} = 0.01$ [11].

In the paper we define the $g-$factors such that the Zeeman shift is equal to

$$E_{\text{Z}} = g\mu_B B M_F, \qquad (2)$$

where M_F is projection of the total angular momentum $\mathbf{F}$ (including nuclear spin) on the direction of $\mathbf{B}$ and the

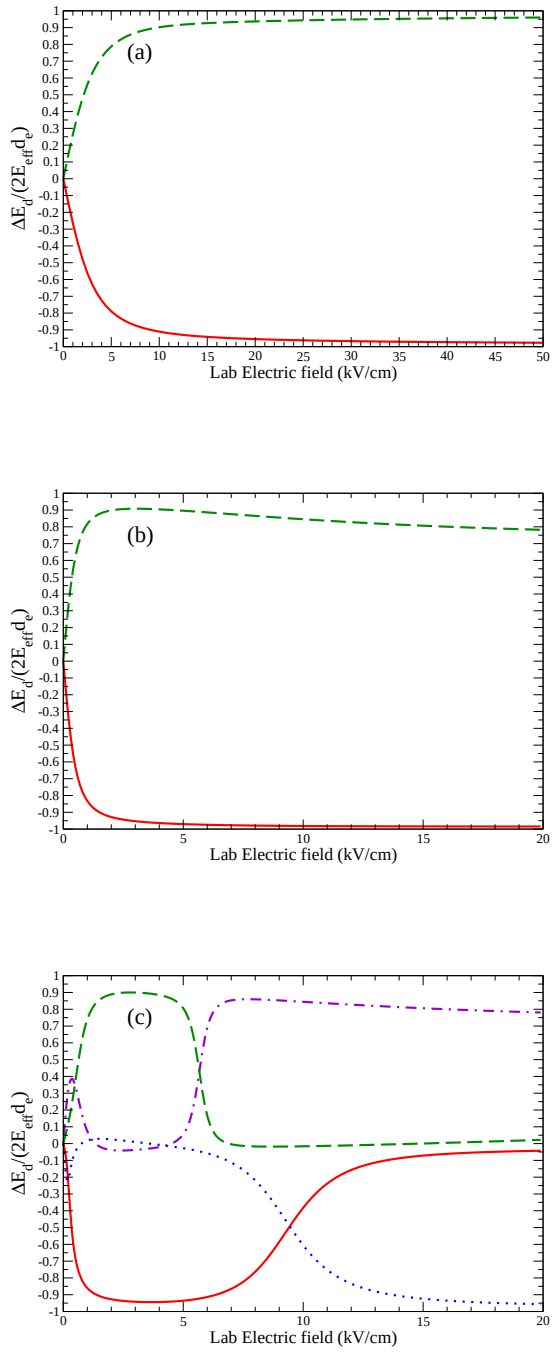

FIG. 3. (Color online) The eEDM induced Stark splitting (ΔE) between $\pm M_F$ pairs of hyperfine states. (a) ^{208}PbF. The solid (red) line corresponds to the $|M_F|$=1 lower lying Ω-doublet states whereas the dashed (green) line corresponds to the higher lying $|M_F|$=1 states. (b) ^{207}PbF. The solid (red) line corresponds to the $|M_F|$=3/2 lower lying Ω-doublet states whereas the dashed (green) line corresponds to the higher lying $|M_F|$=3/2 states. (c) ^{207}PbF. The solid (red) line corresponds to the lower lying F=3/2, $|M_F|$=1/2 Ω-doublet states, the dashed (green) line corresponds to the higher lying F=3/2, $|M_F|$=1/2 states, the dotted (blue) line corresponds to the lower lying F=1/2, $|M_F|$=1/2 states, whereas the dashed-dotted (violet) line corresponds to the higher lying F=1/2, $|M_F|$=1/2 states

electric field, **E**. In Fig. 5, the calculated electric field dependent $g-$factor is presented. From Fig. (5) (a) one can see that taking into account the mixing of different rotational levels by the electric field is important for accurate evaluation of the $g-$factors.

As can be seen in Fig. (3) the advantage of the ^{207}PbF molecule is that it is polarized at a lower electric field and has smaller absolute $g-$factors than does ^{208}PbF. This is important for the eEDM experiment as larger fields and $g-$factors lead to greater systematic uncertainties in experimental measurements. For E = 5 kV/cm the eEDM Stark shift reaches 80% of the maximum value for ^{208}PbF, whereas for ^{207}PbF, $|M_F|$=3/2 the same efficiency is achieved at E = 1 kV/cm, and for E = 2 kV/cm it is 90%. The values for the $g-$factors vary from 0.04 to 0.01. As a comparative example, the YbF molecule with g = 2 the efficiency is only about 55% for E = 10 kV/cm ([26]).

As a posited eEDM splitting ΔE between $\pm M_F$ levels is measured, the eEDM value $d_e = \frac{\Delta E}{2E_{\rm eff}}$ can be extracted. However, according to eq. (2), an external magnetic field also leads to a splitting, i.e. the assumed energy difference between the $+|M_F|$ and $-|M_F|$ levels $\Delta E_Z = 2g\mu_B B|M_F|$. Therefore a stray magnetic field leads to systematic effects, and the smaller the g-factor the smaller the corresponding systematics. The complex hyperfine structure of ^{207}PbF prevents a regular dependence on electric field for both the eEDM Stark shift and the $g-$factor, as shown in Figures (3) and (5). There are several field values for which the $g-$factors are zero or near-zero. However, they are strongly (but not exactly) correlated with zero values for the eEDM Stark shift. For example, for the higher lying F=1/2, $|M_F|$=1/2 states (the dashed-dotted (violet) line) the $g-$factor is equal to zero at E = 0.87 kV/cm, whereas $\Delta E_d = 0.25 d_e E_{\rm eff}$ is small (compared to the maximum value $2d_eE_{\rm eff}$), but nonzero.

An efficient way to suppress the systematics related to the stray magnetic field is possible if we have two different levels which have $\Delta E^1_Z = \Delta E^2_Z$ and opposite eEDM induced splittings $\Delta E^1_d = -\Delta E^2_d$. In this case extracting the eEDM using the formula $d_e = \frac{\Delta E^1 - \Delta E^2}{4E_{\rm eff}}$ will double the eEDM signal and cancel out the contribution from the stray magnetic field. Here $\Delta E^i = \Delta E^i_d + \Delta E^i_Z$ is the total splitting. It has been shown previously that the levels with the required structure are closely-spaced Ω-doublet levels, such as in ThO [16, 18, 27–30] or HfF^+ [31, 32]. Unfortunately Figs. (3) and (5) show that the PbF molecule does not have levels with the required structure. However, certain combinations of the splittings do allow for the cancellation of the Zeeman contribution while keeping a nonzero contribution from the eEDM. For example, if state "1" is the lower

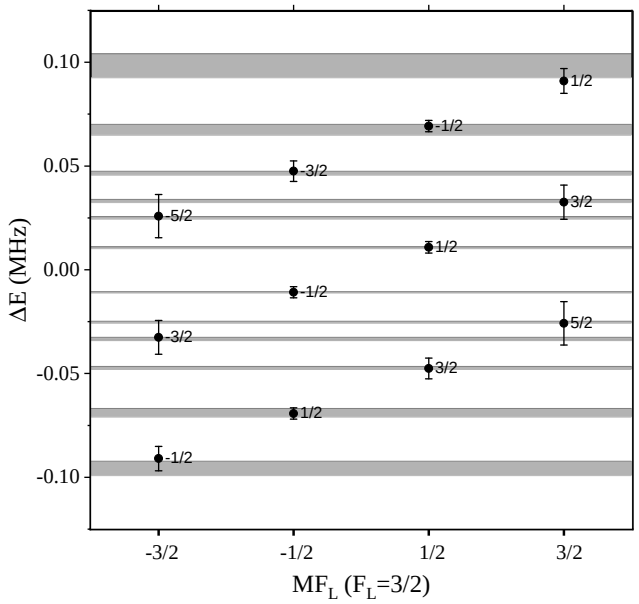

FIG. 4. Calculated (circles) and experimental (horizontal bands, bandwidths corresponding to two standard deviation uncertainty) shifts for the $F_L = 3/2 \rightarrow F_U = 5/2$ transition at $\nu = 22541.912$ MHz. MF_L values are on the x-axis, and MF_U values are marked in the figure. Note the excellent agreement and the eight/four-fold natures of the $\Delta M_F = \pm 1$ and $\Delta M_F = 0$ transitions clearly apparent in Fig. 1.

lying F=3/2, $|M_F|$=1/2 (solid (red) line) and state "2" is the higher lying F=3/2, $|M_F|$=1/2 (dashed (green) line), then for $E = 2$ kV/cm the combination of Zeeman splittings $\Delta E_Z^1 + 2.34\Delta E_Z^2 = 0$ cancels, while the contribution from the eEDM to the same combination $\Delta E_d^1 + 2.34\Delta E_d^2 = 2.3 d_e E_{\rm eff}$ is nonzero.

CONCLUSIONS

Experimental data and theoretical calculations for the $g-$factors of ^{207}Pb^{19}F for the electric field-free case are reported and found to be in a very good agreement with each other and with the body-fixed $g-$factors $G_{\parallel} = 0.081$, $G_{\perp} = -0.27$ obtained in Ref. [11]. The calculated sensitivity to the electron electric dipole moment shows that an electric field of $1-2$ kV/cm is optimal for an experiment. The calculated electric field dependent $g-$factors provide the information needed to control systematic effects related to stray magnetic fields in future experiments such as those capitalizing on the coincidental near-degeneracy of levels of opposite parity in ^{207}PbF.

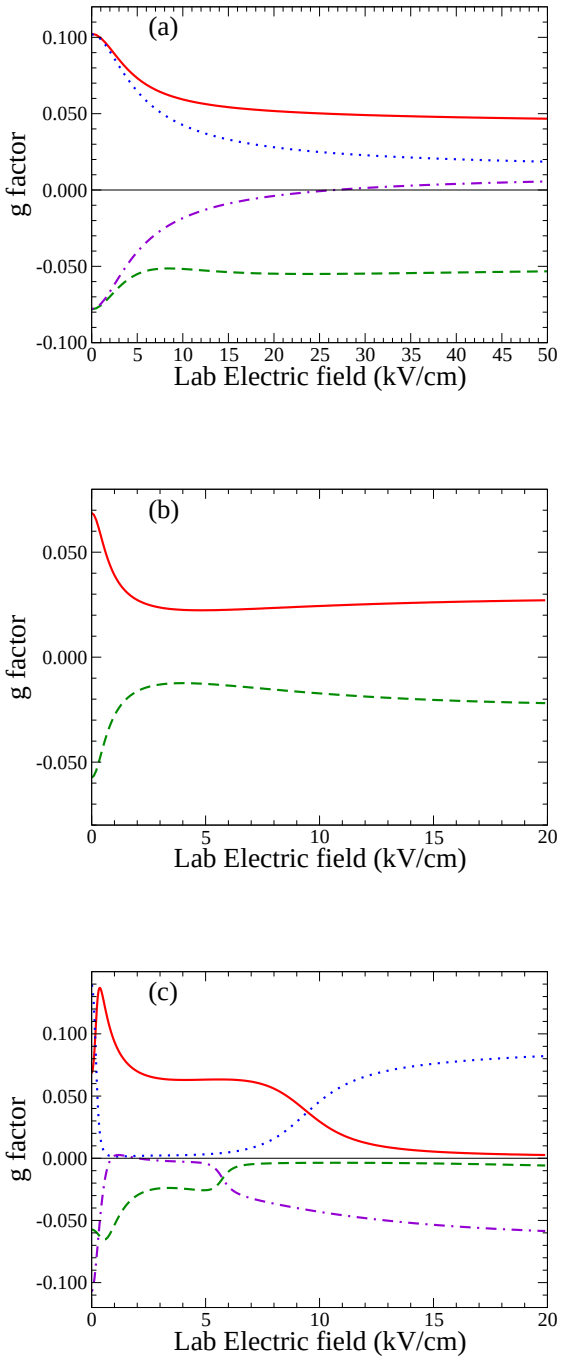

FIG. 5. (Color online) Calculated g-factors. (a) ^{208}PbF. The solid (red) and dotted (blue) lines correspond to the $|M_F|$=1 lower lying Ω-doublet states whereas the dashed (green) and the dashed-dotted (violet) lines correspond to the higher lying $|M_F|$=1 states. The dotted (blue) and the dashed-dotted (violet) lines were calculated without interaction with other rotational levels taken into account. (b) ^{207}PbF. The solid (red) line corresponds to the $|M_F|$=3/2 lower lying Ω-doublet states whereas the dashed (green) line corresponds to the higher lying $|M_F|$=3/2 states. (c) ^{207}PbF. The solid (red) line corresponds to the lower lying F=3/2, $|M_F|$=1/2 Ω-doublet states, the dashed (green) line corresponds to the higher lying F=3/2, $|M_F|$=1/2 states, the dotted (blue) line corresponds to the lower lying F=1/2, $|M_F|$=1/2 states, whereas the dashed-dotted (violet) line corresponds to the higher lying F=1/2, $|M_F|$=1/2 states.

ACKNOWLEDGEMENTS

The authors would like to thank A.L. Baum for his initial preparation of the experimental data and acknowledge Neil Shafer-Ray as a source of inspiration for this series of studies of PbF, dedicating this work in his memory. Molecular calculations were supported by the Russian Science Foundation grant No. 18-12-00227. Work by T. J. Sears was supported by the U.S. Department of Energy, Office of Science, Division of Chemical Sciences, Geosciences and Biosciences within the Office of Basic Energy Sciences, under Award Number DE-SC0018950. R.J. Mawhorter is grateful for research support provided by a Pomona College Sontag Fellowship and Hirsch Research Initiation Grant. P. M. Rupasinghe is grateful for research support provided by SUNY-Oswego Office of Research and Sponsored Programs (ORSP). J.-U. Grabow acknowledges support from the Deutsche Forschungsgemeinschaft grant No. GR 1344 and the Land Niedersachsen.

* petrov_an@pnpi.nrcki.ru; http://www.qchem.pnpi.spb.ru

[1] M. G. Kozlov, V. I. Fomichev, Yu. Yu. Dmitriev, L. N. Labzovsky, and A. V. Titov, J. Phys. B **20**, 4939 (1987).

[2] K. Ziebarth, K. D. Setzer, O. Shestakov, and E. H. Fink, J. Mol. Spectrosc. **191**, 108 (1998), ISSN 0022-2852.

[3] Y. Y. Dmitriev, Y. G. Khait, M. G. Kozlov, L. N. Labzovsky, A. O. Mitrushenkov, A. V. Shtoff, and A. V. Titov, Phys. Lett. A **167**, 280 (1992).

[4] N. E. Shafer-Ray, Phys. Rev. A **73**, 034102 (2006).

[5] C. P. McRaven, P. Sivakumar, and N. E. Shafer-Ray, Phys. Rev. A **78**, 054502(R) (2008), erratum: Phys. Rev. A **80**, 029902(E) (2009).

[6] K. I. Baklanov, A. N. Petrov, A. V. Titov, and M. G. Kozlov, Phys. Rev. A **82**, 060501(R) (2010).

[7] R. J. Mawhorter, B. S. Murphy, A. L. Baum, T. J. S. T. Yang, P. M. Rupasinghe, C. P. McRaven, N. E. Shafer-Ray, L. D. Alphei, and J.-U. Grabow, Phys. Rev. A **84**, 022508 (2011).

[8] L. D. Alphei, J.-U. Grabow, A. N. Petrov, R. Mawhorter, B. Murphy, A. Baum, T. J. Sears, T. Z. Yang, P. M. Rupasinghe, C. P. McRaven, et al., Phys. Rev. A **83**, 040501(R) (2011).

[9] T. Yang, J. Coker, J. E. Furneaux, and N. E. Shafer-Ray, Phys. Rev. A **87**, 014101 (2013).

[10] A. N. Petrov, L. V. Skripnikov, A. V. Titov, and R. J. Mawhorter, Phys. Rev. A **88**, 010501(R) (2013).

[11] L. V. Skripnikov, A. N. Petrov, A. V. Titov, R. J. Mawhorter, A. L. Baum, T. J. Sears, and J.-U. Grabow, Phys. Rev. A **92**, 032508 (2015).

[12] C. P. McRaven, P. Sivakumar, and N. E. Shafer-Ray, Phys. Rev. A **78**, 054502(R) (2008).

[13] V. V. Flambaum, Y. V. Stadnik, M. G. Kozlov, and A. N. Petrov, Phys. Rev. A **88**, 052124 (2013).

[14] A. Borschevsky, M. Iliaš, V. A. Dzuba, V. V. Flambaum, and P. Schwerdtfeger, Phys. Rev. A **88**, 022125 (2013).

[15] R. Mawhorter, J. Munoz-Lopez, Y. Kim, A. Biekert, T. Sears, J.-U. Grabow, A. D. Kudashov, L. V. Skripnikov, A. V. Titov, and A. N. Petrov (2018), to be published, http://meetings.aps.org/link/BAPS.2018.DAMOP.E01.81.

[16] A. N. Petrov, L. V. Skripnikov, A. V. Titov, N. R. Hutzler, P. W. Hess, B. R. O'Leary, B. Spaun, D. DeMille, G. Gabrielse, and J. M. Doyle, Phys. Rev. A **89**, 062505 (2014).

[17] A. N. Petrov, L. V. Skripnikov, and A. V. Titov, Phys. Rev. A **96**, 022508 (2017).

[18] V. Andreev, D. Ang, D. DeMille, J. Doyle, G. Gabrielse, J. Haefner, N. Hutzler, Z. Lasner, C. Meisenhelder, B. O'Leary, et al., Nature **562**, 355 (2018).

[19] J. U. Grabow, W. Stahl, and H. Dreizler, Rev. Sci. Instr. **67**, 4072 (1996).

[20] B. M. Giuliano, L. Bizzocchi, and J. U. Grabow, J. Mol. Spectrosc. **251**, 261 (2008).

[21] A. L. Baum, B.A. thesis, Pomona College, (2010).

[22] A. N. Petrov, Phys. Rev. A **83**, 024502 (2011).

[23] V. Fella, L. V. Skripnikov, W. Nörtershäuser, M. R. Buchner, H. L. Deubner, F. Kraus, A. F. Privalov, V. M. Shabaev, and M. Vogel, Phys. Rev. Research **2**, 013368 (2020).

[24] P. M. Rupasinghe, Ph.D. thesis, University of Oklahoma (2011).

[25] L. V. Skripnikov, A. D. Kudashov, A. N. Petrov, and A. V. Titov, Phys. Rev. A **90**, 064501 (2014).

[26] D. M. Kara, I. J. Smallman, J. J. Hudson, B. E. Sauer, M. R. Tarbutt, and E.-A. Hinds, New Journal of Physics **14**, 103051 (2012).

[27] D. DeMille, F. B. an S. Bickman, D. Kawall, L. Hunter, D. Krause, Jr, S. Maxwell, and K. Ulmer, AIP Conf. Proc. **596**, 72 (2001).

[28] A. C. Vutha, W. C. Campbell, Y. V. Gurevich, N. R. Hutzler, M. Parsons, D. Patterson, E. Petrik, B. Spaun, J. M. Doyle, G. Gabrielse, et al., J. Phys. B **43**, 074007 (2010).

[29] A. N. Petrov, Phys. Rev. A **91**, 062509 (2015).

[30] A. N. Petrov, Phys. Rev. A **95**, 062501 (2017).

[31] W. B. Cairncross, D. N. Gresh, M. Grau, K. C. Cossel, T. S. Roussy, Y. Ni, Y. Zhou, J. Ye, and E. A. Cornell, Phys. Rev. Lett. **119**, 153001 (2017).

[32] A. N. Petrov, Phys. Rev. A **97**, 052504 (2018).